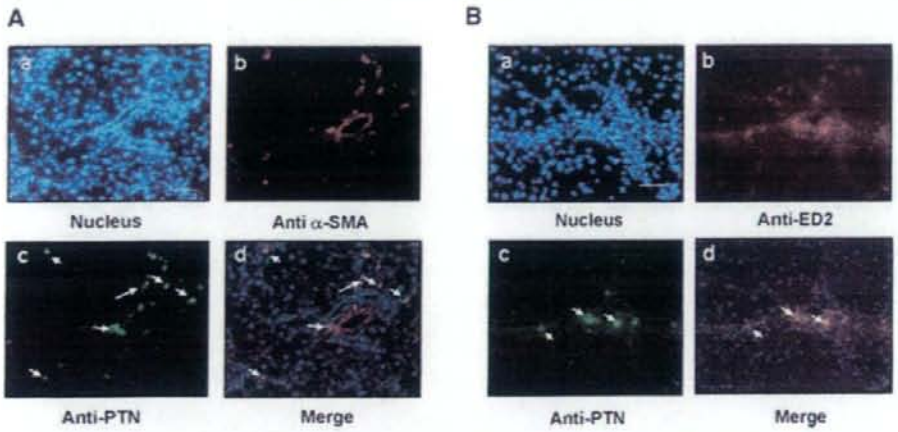

Figure 2. Identification of PTN⁺-cells. Rats were treated with CCl_4 for 8 wk, and their livers were subjected to double immunohistochemistry for PTN and α-SMA (A), and for PTN and ED2 (B). After staining with the antibodies sections were stained with Hoechst 33342 for nuclear staining (a in A and B). Bar represents 100 μm. Arrows indicate the PTN positive nonparenchymal cells.

Geneticin-resistant colonies. These cells were subjected to RT-PCR (Figure 4A) and Western blotting (Figure 4B) for checking the PTN expression at mRNA and protein levels, respectively. The clones all strongly expressed PTN mRNA, Huh-7-C4 and Huh-7-C5 cells showing higher expressions than the remaining two colonies. Null vector-bearing control cells, Huh-7-V cells, expressed it very faintly. Western blotting showed that Huh-7-C5 cells secreted a high level of rPTN and Huh-7-C4 cells secreted it at a detectable level, but Huh-7-C2 and Huh-7-C6 cells did not.

Effects of TGFβ1 on Apoptosis of PTN Gene-Expressing Huh-7 Cells

First we found that there was no significant difference in the proliferate ability between PTN gene-expressing (Huh-7-C4 and Huh-7-C5) and control cells (Huh-7-V cells) (Figure 4C). Next, we evaluated the TGFβ1 effect on the PTN transfected cells: Huh-7-C4 and Huh-7-C5 cells were cultured for up to 3 d in the presence of three different concentrations of TGFβ1 (1, 5, and 10 ng/ml) and the cell number was counted (Figure 4D). Similarly, Huh-7-V cells were cultured as control cells. TGFβ1 significantly decreased the cell number of Huh-7-V cells in dose- and the culture length-dependent manners (open bars in Figure 4D). In contrast, Both Huh-7-C4 and Huh-7-C5 cells similarly resisted this effect of TGFβ1.

We identified the apoptotic cells at 3 d in the above cultures with 10 ng/ml TGFβ1 by Hoechst- (Figure 4E,a and c) and TUNEL-staining (Figure 4E,d and f). It was apparent that TGFβ1-induced apoptotic cells were significantly decreased in both Huh-7-C4 (Figure 4E,b and e) and -C5 (Figure 4E,c and f) compared to the control cells (Figure 4E,a and d). The number of the apoptotic cells was counted for each of the TUNEL-stained cells and their incidence is shown in Figure 4F. The ratio of apoptotic cells in both clones bearing PTN-genes was decreased to approximately 25% of the control cells.

Figure 3. (*Overlesf*) Suppression of TGFβ-induced apoptosis in hepatoma cells by PTN. (A) Effects of PTN on the growth of cells of cancer cell line and normal hepatocytes. Cells of Huh-7, HepG2, and primary rat hepatocytes, 5×10^3 cells each, were seeded in 12 well plates and treated with 100 ng/ml of rPTN for 1 wk. rPTN increased the proliferation of HepG2 cells and normal rat hepatocytes, but not Huh-7 cells. The same experiment was repeated 3 times and the results are presented as the mean ± SD. (B) The effects of PTN on the cell viability. Huh-7 cells were treated with 0, 1, and 2 ng/ml of rTGFβ1 with or without 100 ng/ml of rPTN for up to 3 d. The number of the cells was counted at 2 and 3 d in culture and the results are shown as % of the number of the cells that had no treatment. The open bars represent the cultures in the presence of TGFβ1 at the indicated concentrations, but in the absence of rPTN. The closed bars are for the cultures in the presence of both TGFβ1 and rPTN. (C) Apoptotic changes in nuclear chromatins of Huh-7 cells. The cells at 2 d with 2 ng/ml TGFβ1 and 100 ng/ml rPTN each alone or together shown in (B) were stained with Hoechst 33342 to examine the apoptotic changes in nuclear chromatins. (a) Cells without cytokines. (b) Cells with 2 ng/ml TGFβ1. (c) Cells with 100 ng/ml rPTN. (d) Cells with both 2 ng/ml TGFβ1 and 100 ng/ml rPTN. Bar represents 100 μm. (D) The incidences of apoptosis of the cultured Huh-7 cells. The number of the apoptotic cells was counted in (C) and divided by the total cells in the tested field to obtain the apoptosis rate (%). "No Tx" represents the cells without treatment. * represents the statistical significance at $P<0.05$ between "TGFβ1" and "PTN and TGFβ1". (E) Apoptotic changes in nuclear chromatins of normal rat hepatocytes. The cells at 2 d with 2 ng/ml TGFβ1 and 100 ng/ml rPTN each alone or together were stained with Hoechst 33342 as in (C). (a) Cells without cytokines. (b) Cells with 2 ng/ml TGFβ1. (c) Cells with 100 ng/ml rPTN. (d) Cells with both 2 ng/ml TGFβ1 and 100 ng/ml rPTN. Bar represents 100 μm. (F) The incidences of apoptosis of the rat hepatocytes. The apoptosis rate (%) was calculated as in (D). * represents the statistical significance at a $P<0.05$ level between TGFβ1 treatment versus TGFβ1 and rPTN co-treatment.

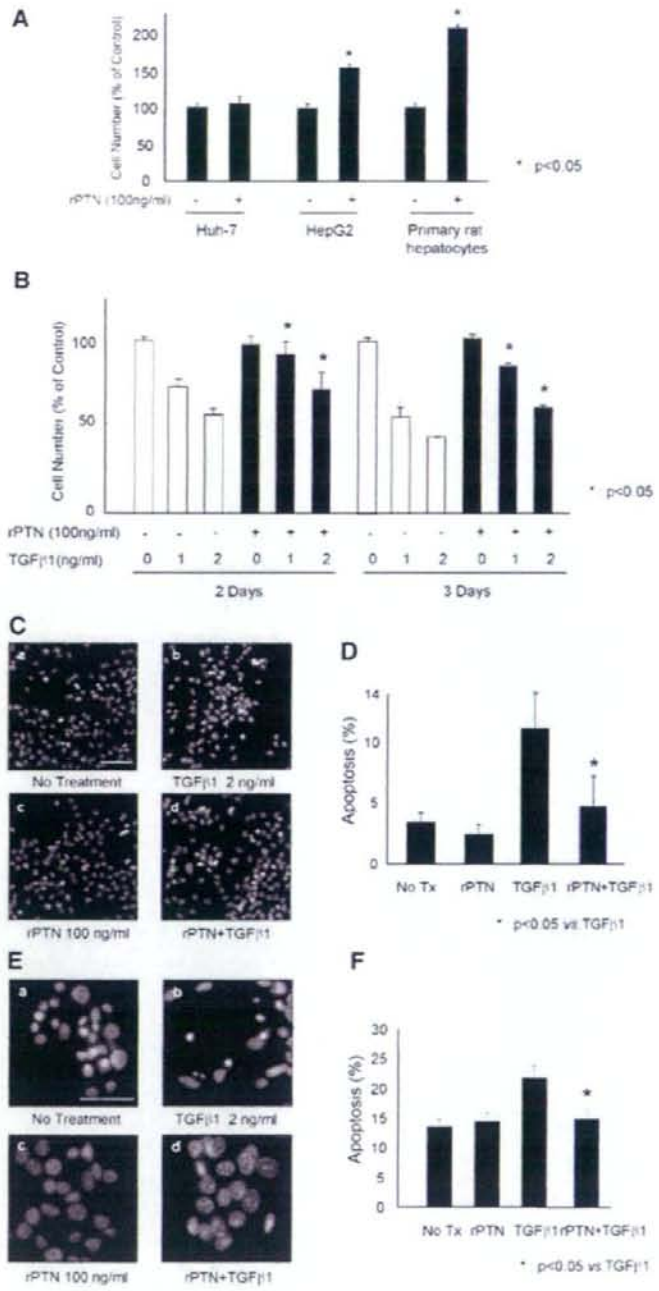
A
Cell Number (% of Control)
200
150
100
50
0
* p<0.05
rPTN (100ng/ml) - + - + - +
Huh-7
HepG2
Primary rat hepatocytes
B
Cell Number (% of Control)
100
50
0
* p<0.05
rPTN (100ng/ml) - - - + + + - - - + + +
TGFβ1(ng/ml) 0 1 2 0 1 2 0 1 2 0 1 2
2 Days
3 Days
C
No Treatment
TGFβ1 2 ng/ml
rPTN 100 ng/ml
rPTN+TGFβ1
D
Apoptosis (%)
14
10
5
0
No Tx rPTN TGFβ1 rPTN+TGFβ1
* p<0.05 vs TGFβ1
E
No Treatment
TGFβ1 2 ng/ml
rPTN 100 ng/ml
rPTN+TGFβ1
F
Apoptosis (%)
30
25
20
15
10
5
0
No Tx rPTN TGFβ1 rPTN+TGFβ1
* p<0.05 vs TGFβ1

Figure 3.

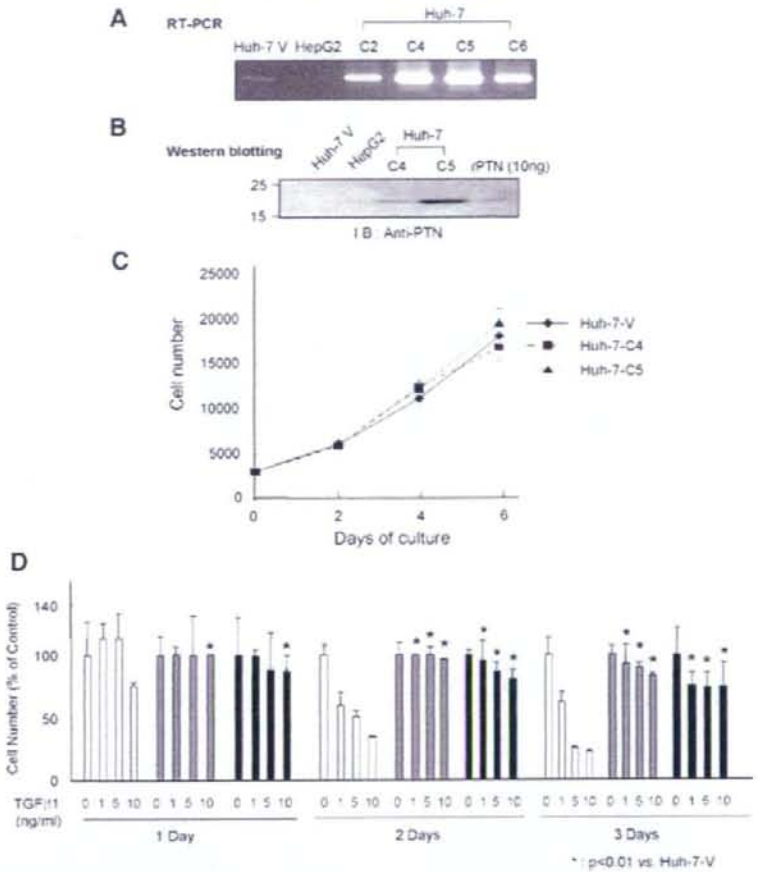

Figure 4. Effects of TGFβ1 on PTN-expressing Huh-7 cells. (A) Establishment of PTN gene-expressing Huh-7 cells. Huh-7 cells were transfected with pcDNA3 vectors bearing PTN cDNA, which yielded four single cell colonies, Huh-7-C2, Huh-7-C4, Huh-7-C5, and Huh-7-C6. Expression levels of PTN mRNA and protein were determined by RT-PCR (A) and Western blotting (B), respectively. Similarly, the expression levels were determined for Huh-7-V and HepG2 cells. Huh-7-V cells weakly expressed PTN mRNA, but HepG2 cells did not. Huh-7-C2, -C4, -C5, and -C6 expressed PTN mRNA, but only Huh-7-C4 and Huh-7-C5 cells secreted PTN protein in culture media at detectable levels. The molecular masses are shown at the left side of the gel. The most right lane was for 10 ng of standard rPTN. (C) Growth of PTN gene-expressing Huh-7 cells. Huh-7-V, Huh-7-C4, and Huh-7-C5, 3×10^5 cells each, were seeded in 24-well plates and cultured for 6 d. Cells were harvested at 2, 4, and 6 d of culture for cell count. The same experiment was repeated 3 times and the results are presented as the mean ± SD. (D) Effects of TGFβ1 on PTN-expressing Huh-7 cells. Huh-7-V, -C4, and -C5 cells were cultured up to 3 d in the presence of 0, 1, 5, and 10 ng/ml. The cell number was counted at 1, 2, and 3 d in culture and the cell number ratio (%) was calculated as in Figure 3B. The open, gray, and black bars represent Huh-7-V, -C4, and -C5 cells, respectively. * represents the statistical significance at a $P < 0.01$ level between Huh-7-V versus Huh-7-C4 and -C5 cells. (E) Identification of apoptotic cells in cultures. Huh-7-V (a and d), -C4 (b and e), and -C5 cells (c and f) were cultured for 3 d in the presence of 10 ng/ml TGFβ1 and stained with Hoechst (a–c) or with TUNEL (d–f). Bar represents 100 μm. (F) The apoptotic cell ratio was determined by dividing the number of the TUNEL$^+$-cells with that of the total number in the examined field. Each number was obtained from photos shown in (E,d–f). * represents the statistical significance at a $P < 0.01$ level between Huh-7-V versus Huh-7-C4 and -C5 cells. (G) The cell viability in the presence of mitomycin C. Huh-7-V, -C4, and -C5 cells were cultured for 2 d as in C except that TGFβ1 was replaced with mitomycin C at the indicated concentrations. The three differently colored bars represent cell species as in (C). (H) Suppression of TGFβ1-induced apoptosis in Huh-7-C5 conditioned media. Huh-7-V and Huh-7-C5 cells, 5×10^5 cells each, were seeded in 100 mm dishes and cultured for 2 d. The culture media were collected and used as the conditioned media. Huh-7 cells were cultured in the conditioned media from Huh-7-C5 or Huh-7-V in the presence of 2 ng/ml TGFβ1. CM: conditioned media. (I) The incidences of apoptosis of the Huh-7 cell. The number of the apoptotic cells was counted on photographs shown H and the apoptosis rate (%) was obtained as in E.

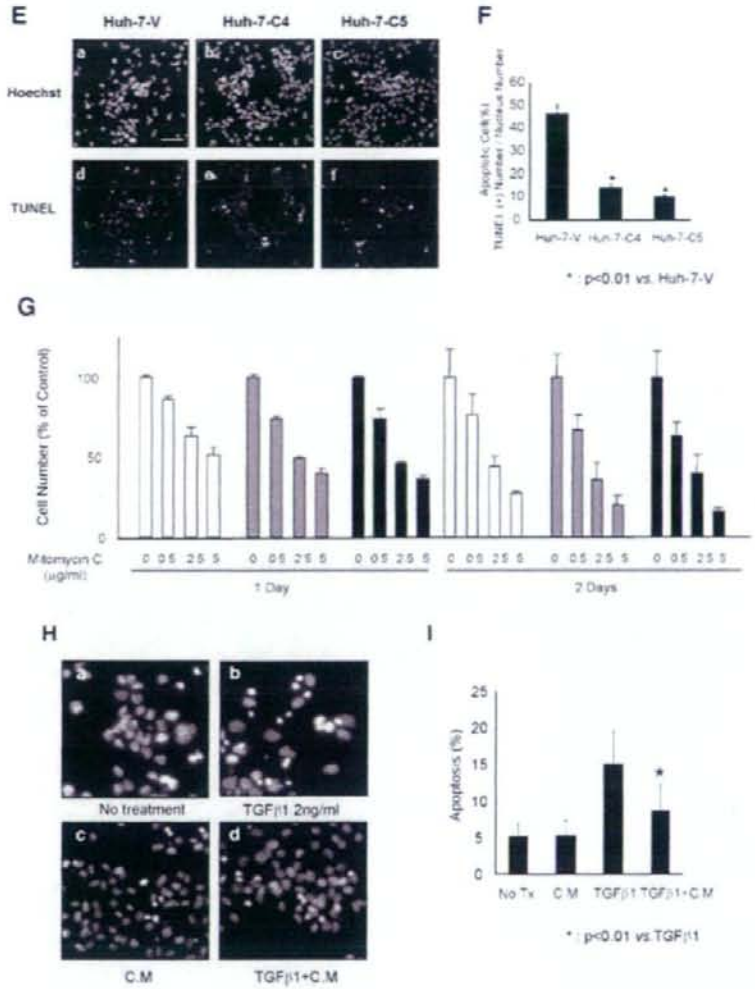

Figure 4. (*Continued*)

In order to exclude the possibility that this anti-apoptotic effect of PTN is a merely non-specific action, we induced the apoptosis on each of these cells with mitomycin-C at concentrations from 0.5 to 5 μg/ml and examined the change in cell number as a measure of apoptosis (Figure 4G). There were no differences in the rate of the cell number decrease among the cells, indicating that PTN specifically inhibit TGFβ1-mediates cell death. The results strongly suggested that PTN secreted by PTN gene-expressing Huh-7 cells suppresses the TGFβ1-induced apoptosis. To further test this suggestion, we examined the effect of conditioned media from the Huh-7-C5 on the TGFβ1-induced apoptosis. Huh-7 cells were cultured in the conditioned media in the presence of 2 ng/ml of TGFβ1 for 3 d. Hoechst staining showed that the conditioned medium apparently inhibited the TGFβ1-induced apoptosis (Figure 4H), which was supported by the quantitative analysis in which the number of the apoptotic cells was counted on the photographs in Figure 4H to calculate the incidence of apoptosis (Figure 4I).

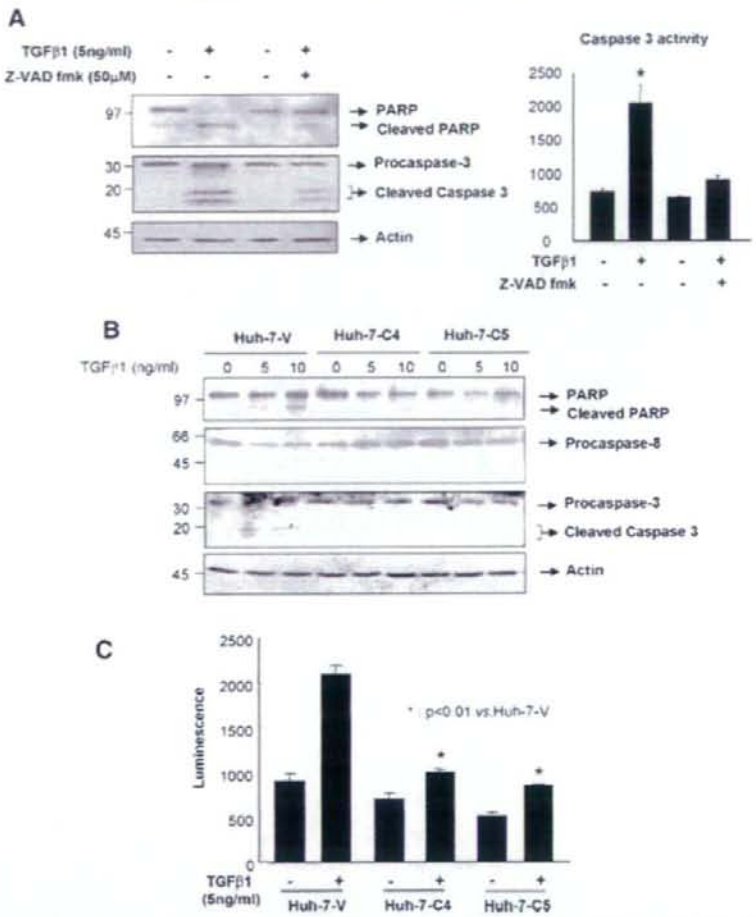

Figure 5. Suppression of TGFβ1-induced activation of caspase-8 and caspase-3 by PTN. (A) Activation of caspase-3 by TGFβ1 in Huh-7 cells. The cells were cultured in the absence (–) or presence (+) of 5 ng/ml TGFβ1 and 50 μM Z-VAD-FMK for 3 d. The cell lysates were prepared from each of the cultured cells and subjected to Western blotting for PARP and procaspase-3 (left panel) and to measurement of caspase-3 activity (right panel). The Arabic numerals at the left side of the gel represent molecular masses. (B) Suppression of TGFβ1-induced cleavage of cellular PARP, pro-caspase-8, and pro-caspase 3 in PTN gene-expressing Huh-7 cells. Huh-7-V, -C4, and -C5 cells were cultured for 3 d in the absence and the presence of 5 and 10 ng/ml TGFβ1. The whole cell lysates of each of the cells was subjected to Western blotting for PARP, caspase-8, caspase-3, and actin. (C) Suppression of TGFβ1-induced caspase-3 activity in Huh-7 cells bearing PTN gene. The whole lysates of the cells in B were used for determining the caspase-3 activity. * represents the statistical significance at $P < 0.01$ level between TGFβ1 treated Huh-7-V versus TGFβ1-treated Huh-7-C4 and -C5 cells.

Inhibition of TGFβ1-Induced Caspase-3 Activation by PTN

The activation of caspase cascades has been known as an essential molecular event in the TGFβ1-induced apoptosis [24]. We investigated an aspect of the mechanism of PTN action on TGFβ1-induced apoptosis targeting the caspase activation. First, we examined the activation of caspase-3 by TGFβ1 in Huh-7 cells (Figure 5A). The cells were cultured in the absence or presence of 5 ng/ml TGFβ1 and Z-VAD-FMK, a caspase inhibitor, for 3 d. The cell lysates were subjected to Western blotting for PARP and procaspase-3 (Figure 5A, left panel). The bands corresponding to the cleaved products of PARP and procaspase-3 were clearly visible. The caspase-3 activity was measured in the cell lysates (Figure 5A, right panel), which quantitatively demonstrated that rTGFβ1 stimulated the activity and Z-VAD-FMK suppressed the rTGFβ1-induced activity.

We examined the TGFβ1-induced apoptosis in PTN-expressing Huh-7 cells. Huh-7-V, Huh-7-C4, and -C5 cells were cultured in the presence of TGFβ1 for 3 d and their cell lysates were Western blotted for PARP, capase-8, and -3 (Figure 5B). rTGFβ1 also induced the cleavage of PARP, procaspase-8 and procaspase-3 in Huh-7-V cells. However, there were no such processed products in Huh-7-C4 and -C5 cells. Actually, the treatment of Huh-7-V cells with rTGFβ1 enhanced the caspase-3 activity (Figure 5C). The extent of the activation was much less in Huh-7-C4 and -C5 cells, supporting the idea that PTN has the suppressive activity on TGFβ1-induced apoptosis.

The anti-apoptotic function of PTN was further tested using FaO rat hepatoma cells, which are also highly sensitive to TGFβ1 in apoptosis induction [30]. Both FaO and Huh-7 cells were transduced with adenovirus vectors carrying PTN gene (PTN-Ad). It was shown that these cells secreted PTN proteins in culture media (Figure 6A). The cells were then treated with 5 ng/ml rTGFβ1 for 2 or 3 d. As shown in Figure 6B and C both types of cells became reluctant to activate caspase-3 in response to TGFβ1 when transfected with PTN gene. These results strongly support that PTN suppresses TGFβ1-induced caspase 3 activation and apoptosis.

DISCUSSION

Studies abundantly accumulated hitherto indicate that the signaling between hepatocytes and HSCs plays a crucial role in regulating normal and abnormal growth of hepatocytes [31]. Especially the role of HSCs in the hepatic fibrogenesis and carcinogenesis has been a major issue among investigators [32]. Previously, we showed that HSC-derived PTN plays a role as a hepatocytes growth factor [6,9]. Furthermore, we showed that PTN

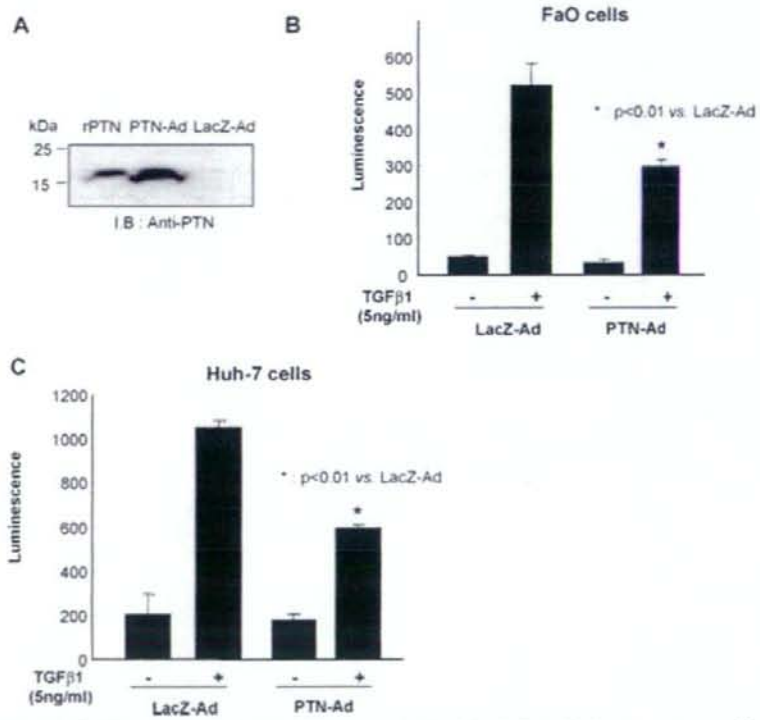

Figure 6. Reluctance of PTN-transgenic cells in responding to TGFβ1. FaO and Huh-7 cells were exposed to PTN- or LacZ-Ad for 3 d and then treated with TGFβ1. (A) Expression of rPTN proteins by the transgenic cells. The culture media were collected from the cell cultures and passed through a heparin gel column. The absorbed proteins were Western blotted with antibodies against PTN. Left, middle, and right lanes were for standard rPTN (10 ng), FaO cells transfected with PTN-Ad, and those with LacZ-Ad, respectively. (B) Suppression of TGFβ1-induced caspase-3 activation in the FaO cells bearing PTN-Ad. The whole lysates were prepared from the above cells for measuring the caspase-3 activity. The symbols, – and +, indicate the absence and presence of 5 ng/ml TGFβ1. (C) Suppression of TGFβ1-induced caspase-3 activation in the Huh-7 cells bearing PTN-gene. Caspase-3 activity was measured for Huh-7 cells as in B. * represents the statistical significance at a $P < 0.01$ level between TGFβ1-treated FaO or Huh-7 cells with LacZ-Ad versus TGFβ1-treated FaO or Huh-7 cells with PTN-Ad.

expression was increased in CCl_4-induced fibrotic liver [10], suggesting the involvement of PTN in hepatic fibrogenesis, to which TGFβ1 is also committed as an anti-hepatocyte growth factor and an ECM-formation accelerator. These previous studies were the major motivation of the present study and we investigated the mechanism of the action of PTN in liver fibrogenesis and carcinogenesis. As a result, we confirmed the previous studies that HSCs and also hepatocytes later increased PTN mRNA expressions during CCl_4-induced liver fibrosis. This confirmation strengthens the previous suggestion that PTN plays a role in liver fibrogenesis.

In this study the role of PTN in hepatic carcinogenesis was tested utilizing known TGFβ1-sensitive human and rat hepatoma cells, Huh-7 and FaO cells, respectively. These cells undergo apoptosis when stimulated by TGFβ1 [30]. We were able to demonstrate that PTN acts as an anti-apoptotic factor. Interestingly, this activity appears to be specific to the TGFβ1-induced apoptosis, because PTN did not show any effect on mitomycin C-induced hepatocyte apoptosis. Caspase-3 is known as a main executor of cell death [33]. It is most likely that PTN suppresses the activation of caspase-8 and cannot activate the caspase-3. We noticed that the extent of the suppression of caspase-3 activity in PTN-Ad-bearing Huh-7 cells (Figure 6C) was lower than that in Huh-7-C4 and -5 (Figure 5C). The PTN-expression by the former cells was transient, peaking at 3 d after infection and was terminated at 7 d (data not shown). In the experiment with PTN-Ad-bearing Huh-7 cells, the cells were treated with TGFβ1 for 3 d from 3 to 6 d post-infection, during which the PTN expression level was considered to be apparently much decreased. This decrease might explain the difference between the suppression levels in the two experiments.

Such an anti-apoptotic effect of PTN appears to be important in hepatocarcinogenesis, because chemically altered hepatocytes undergo the apoptotic pathway through the action of several cytokines in the process of carcinogenesis. It is conceivable that transformed hepatocytes exposed to TGFβ1 are on the two possible paths, one for undergoing apoptosis and the other for escaping from the apoptosis. It is suggested that the cells are capable of "successfully" escaping from the TGFβ1-induced apoptosis under a "favorable" signal such as PTN in this case. Such possibility has earlier been investigated in the chemically induced carcinogenesis in rat liver [21].

TGFβ1 has been shown to be an inhibitor of hepatocyte proliferation as well as a potent inducer of apoptosis in vitro and in vivo, when administered at a high dose, thus indicating that this cytokine can induce regression of rat livers [34,35]. The level of TGFβ1 in liver and serum is increased in the chemically induced liver cirrhosis and carcinogenesis in humans as well as rats [21]. Blocking of TGFβ1 by TGFβ1 type II receptor dominant negative or TGFβ1 soluble antibodies inhibits the fibrosis in dimethylnitrosamine-induced liver fibrosis [19,36]. Furthermore, the hepatocyte proliferation was enhanced in the absence of TGFβ type II receptor in chemically induced hepatocarcinogenesis [21]. Several studies suggest that TGFβ1 is a potent activator of hepatocyte apoptosis and the loss of TGFβ1 signal activates hepatocyte proliferation and hepatocarcinogenesis. These studies all suggest TGFβ1 as one of the potent apoptotic factors working in liver fibrogenesis and carcinogenesis. We propose from the results obtained in the present study that PTN plays a role to protect transforming hepatocytes from apoptosis by suppressing the activity of TGFβ1. However, the effect of PTN on the promoting activity of ECM production, another major activity of TGFβ1, during liver fibrogenesis and carcinogenesis was not tested in the present study and remains to be clarified.

We showed the anti-apoptosis activity of PTN in two different experiments: one was that both rPTN and rTGFβ1 were introduced in cultures of Huh-7 cells with different concentration combinations and the other was that rTGFβ1 was introduced at various concentrations in culture media of PTN-gene transgenic Huh-7 and FaO cells. Anti-apoptotic effect of rPTN was only seen when the cells were treated with in <5 ng/ml of rTGFβ1 in the former experiment. When treated with >5 ng/ml rTGFβ1, the cells were unable to escape from the apoptosis. Furthermore, the effective inhibition of the apoptosis was seen when the concentration of rPTN was >100 ng/ml (data not shown). This might be partly a reflection of the instability of rPTN in the culture media. PTN gene-expressing cell lines were more resistant against the TGFβ1-induced apoptosis. The activation of procaspase-3 did not occur in these cells even at 10 ng/ml of rTGFβ1. Furthermore, PTN-Ad also protected Huh-7 and FaO cells from TGFβ1-induced apoptosis at 5 ng/ml of rTGFβ1. These results indicate that the continuous presence of PTN is more effective than its transient presence.

The present study has made two contributions to the understanding of biological roles of PTN. Firstly, in this study we show that PTN is largely expressed in HSCs and Kupffer cells, and also in some of hepatocytes during liver fibrosis. Secondly, the presence of PTN makes cells resistant to TGFβ1-induced cell death through the inhibition of caspase 3 activation. In summary, PTN is involved in hepatocarcinogenesis and has an anti-apoptotic activity against TGFβ1.

ACKNOWLEDGMENTS

This work was supported by grants from Hiroshima University 21st Century COE Program and CLUSTER, Japan, and was supported by the 2006 grant from Ajou University School of Medicine.

REFERENCES

1. Deuel TF, Zhang N, Yeh HJ, Silos-Santiago I, Wang ZY. Pleiotrophin: A cytokine with diverse functions and a novel signaling pathway. Arch Biochem Biophys 2002;397:162–171.
2. Milner PG, Li YS, Hoffman RM, Kodner CM, Siegel NR, Deuel TF. A novel 17 kD heparin-binding growth factor (HBGF-8) in bovine uterus: Purification and N-terminal amino acid sequence. Biochem Biophys Res Commun 1989;165: 1096–1103.
3. Li YS, Milner PG, Chauhan AK, et al. Cloning and expression of a developmentally regulated protein that induces mitogenic and neurite outgrowth activity. Science 1990; 250:1690–1694.
4. Kadomatsu K, Tomomura M, Muramatsu T. cDNA cloning and sequencing of a new gene intensely expressed in early differentiation stages of embryonal carcinoma cells and in mid-gestation period of mouse embryogenesis. Biochem Biophys Res Commun 1988;151:1312–1318.
5. Laaroubi K, Delbe J, Vacherot F, et al., Mitogenic and in vitro angiogenic activity of human recombinant heparin affin regulatory peptide. Growth Factors 1994;10:89–98.
6. Asahina K, Sato H, Yamasaki C, et al. Pleiotrophin/heparin-binding growth-associated molecule as a mitogen of rat hepatocytes and its role in regeneration and development of liver. Am J Pathol 2002;160:2191–2205.
7. Chauhan AK, Li YS, Deuel TF. Pleiotrophin transforms NIH 3T3 cells and induces tumors in nude mice. Proc Natl Acad Sci USA 1993;90:679–682.
8. Chen H, Gordon MS, Campbell RA, et al. Pleiotrophin is highly expressed by myeloma cells and promotes myeloma tumor growth. Blood 2007;110:287–295.
9. Sato H, Funahashi M, Kristensen DB, Tateno C, Yoshizato K. Pleiotrophin as a Swiss 3T3 cell-derived potent mitogen for adult rat hepatocytes. Exp Cell Res 1999;246:152–164.
10. Kohashi T, Tateaki Y, Tateno C, Asahara T, Obara M, Yoshizato K. Expression of pleiotrophin in hepatic non-parenchymal cells and preneoplastic nodules in carbon tetrachloride-induced fibrotic rat liver. Growth Factors 2002;20:53–60.
11. Hsu IC, Metcalf RA, Sun T, Welsh JA, Wang NJ, Harris CC. Mutational hotspot in the p53 gene in human hepatocellular carcinomas. Nature 1991;350:427–428.
12. Moriya K, Fujie H, Shintani Y, et al. The core protein of hepatitis C virus induces hepatocellular carcinoma in transgenic mice. Nat Med 1998;4:1065–1067.
13. Thorgeirsson SS, Teramoto T, Factor VM. Dysregulation of apoptosis in hepatocellular carcinoma. Semin Liver Dis 1998; 18:115–122.
14. Bataller R, Brenner DA. Liver fibrosis. J Clin Invest 2005;115: 209–218.
15. Miwa Y, Harrison PM, Farzaneh F, Langley PG, Williams R, Hughes RD. Plasma levels and hepatic mRNA expression of transforming growth factor-beta1 in patients with fulminant hepatic failure. J Hepatol 1997;27:780–788.
16. Carr BI, Hayashi I, Branum EL, Moses HL. Inhibition of DNA synthesis in rat hepatocytes by platelet-derived type beta transforming growth factor. Cancer Res 1986;46:2330–2334.
17. Strain AJ, Frazer A, Hill DJ, Milner RD. Transforming growth factor beta inhibits DNA synthesis in hepatocytes isolated from normal and regenerating rat liver. Biochem Biophys Res Commun 1987;145:436–442.
18. Caja L, Ortiz C, Bertran E, et al. Differential intracellular signaling induced by TGF-beta in rat adult hepatocytes and hepatoma cells: Implications in liver carcinogenesis. Cell Signal 2007;19:683–694.
19. Nakamura T, Sakata R, Ueno T, Sata M, Ueno H. Inhibition of transforming growth factor beta prevents progression of liver fibrosis and enhances hepatocyte regeneration in dimethylnitrosamine-treated rats. Hepatology 2000;32: 247–255.
20. Park YN, Chae KJ, Kim YB, Park C, Theise N. Apoptosis and proliferation in hepatocarcinogenesis related to cirrhosis. Cancer 2001;92:2733–2738.
21. Lim IK, Park SC, Song KY, et al. Regulation of selection of liver nodules initiated with N-nitrosodiethylamine and promoted with nodularin injections in fischer 344 male rats by reciprocal expression of transforming growth factor-beta1 and its receptors. Mol Carcinog 1999;26:83–92.
22. Fan G, Ma X, Kren BT, Steer CJ. The retinoblastoma gene product inhibits TGF-beta1 induced apoptosis in primary rat hepatocytes and human HuH-7 hepatoma cells. Oncogene 1996;12:1909–1919.
23. Black D, Lyman S, Qian T, et al. Transforming growth factor beta mediates hepatocyte apoptosis through Smad3 generation of reactive oxygen species. Biochimie 2007;89: 1464–1473.
24. Shima Y, Nakao K, Nakashima T, et al. Activation of caspase-8 in transforming growth factor-beta-induced apoptosis of human hepatoma cells. Hepatology 1999;30:1215–1222.
25. Tateno C, Takai-Kajihara K, Yamasaki C, Sato H, Yoshizato K. Heterogeneity of growth potential of adult rat hepatocytes in vitro. Hepatology 2000;31:65–74.
26. Kristensen DB, Kawada N, Imamura K, et al. Proteome analysis of rat hepatic stellate cells. Hepatology 2000; 32: 268–277.
27. Tewari M, Quan LT, O'Rourke K, et al. Yama/CPP32 beta, a mammalian homolog of CED-3, is a CrmA-inhibitable protease that cleaves the death substrate poly(ADP-ribose) polymerase. Cell 1995;81:801–809.
28. Czaja MJ, Weiner FR, Flanders KC, et al. In vitro and in vivo association of transforming growth factor-beta 1 with hepatic fibrosis. J Cell Biol 1989;108:2477–2482.
29. Armendariz-Borunda J, Seyer JM, Kang AH, Raghow R. Regulation of TGF beta gene expression in rat liver intoxicated with carbon tetrachloride. FASEB J 1990;4: 215–221.
30. Lim IK, Joo HJ, Choi KS, et al. Protection of 5alpha-dihydrotestosterone against TGF-beta-induced apoptosis in FaO cells and induction of mitosis in HepG2 cells. Int J Cancer 1997;72:351–355.
31. Gressner AM, Lahme B, Brenzel A. Molecular dissection of the mitogenic effect of hepatocytes on cultured hepatic stellate cells. Hepatology 1995;22:1507–1518.
32. Lissoos TW, Davis BH. Pathogenesis of hepatic fibrosis and the role of cytokines. J Clin Gastroenterol 1992;15:63–67.
33. Nicholson DW, Ali A, Thornberry NA, et al. Identification and inhibition of the ICE/CED-3 protease necessary for mammalian apoptosis. Nature 1995;376:37–43.
34. Schulte-Hermann R, Bursch W, Kraupp-Grasl B, Oberhammer F, Wagner A. Programmed cell death and its protective role with particular reference to apoptosis. Toxicol Lett 1992;64–65:569–574.
35. Oberhammer F, Bursch W, Tiefenbacher R, et al. Apoptosis is induced by transforming growth factor-beta 1 within 5 hours in regressing liver without significant fragmentation of the DNA. Hepatology 1993;8:1238–1246.
36. George J, Roulot D, Koteliansky VE, Bissell DM. In vivo inhibition of rat stellate cell activation by soluble transforming growth factor beta type II receptor: A potential new therapy for hepatic fibrosis. Proc Natl Acad Sci USA 1999; 96:12719–12724.

Develop. Growth Differ. (2008) **50**, 307–320 doi: 10.1111/j.1440-169x.2008.01034.x

Original Article

Identification and characterization of nucleoplasmin 3 as a histone-binding protein in embryonic stem cells

Natsuki Motoi,[1,2] Ken-ichi Suzuki,[1,2] Ryuichi Hirota,[3†] Penny Johnson,[4] Ken Oofusa,[3‡] Yutaka Kikuchi,[1] and Katsutoshi Yoshizato[1,2*§]

[1]*Developmental Biology Laboratory and* [2]*Hiroshima University 21st Century COE Program for Advanced Radiation Casualty Medicine, Department of Biological Science, Graduate School of Science, Hiroshima University, 1-3-1 Kagamiyama, Higashihiroshima, Hiroshima 739-8526,* [3]*ProPhoenix Company, 3-13-26, Kagamiyama, Higashihiroshima, Hiroshima 739-0046, Japan; and* [4]*Intercytex Company, Grafton Street, Manchester, M13 9XX, UK*

Embryonic stem (ES) cells are thought to have unique chromatin structures responsible for their capacity for self-renewal and pluripotency. To examine this possibility, we sought nuclear proteins in mouse ES cells that specifically bind to histones using a pull-down assay with synthetic peptides of histone H3 and H4 tail domain as baits. Nuclear proteins preferentially bound to the latter. We identified 45 proteins associated with the histone H4 tail and grouped them into four categories: 10 chromatin remodeling proteins, five histone chaperones, two histone modification-related proteins, and 28 other proteins. mRNA expression levels of 20 proteins selected from these 45 proteins were compared between undifferentiated and retinoic acid (RA)-induced differentiated ES cells. All of the genes were similarly expressed in both states of ES cells, except nucleoplasmin 3 (NPM3) that was expressed at a higher level in the undifferentiated cells. NPM3 proteins were localized in the nucleoli and nuclei of the cells and expression was decreased during RA-induced differentiation. When transfected with NPM3 gene, ES cells significantly increased their proliferation compared with control cells. The present study strongly suggests that NPM3 is a chromatin remodeling protein responsible for the unique chromatin structure and replicative capacity of ES cells.

Key words: chromatin remodeling, histone chaperone, histone modification, histone tail, retinoic acid.

Introduction

Embryonic stem (ES) cells are derived from the inner cell mass in mammalian blastocysts and possess two unique characteristics: self-renewal, the activity of unlimited cell propagation, and pluripotency, the capability to differentiate into multilineage cell types through various differentiation processes (Evans & Kaufman 1981).

Mouse ES cells require leukemia inhibitory factor (LIF) (Williams *et al.* 1988) in order to exhibit these unique characteristics. Researchers have reported several transcription factors that are involved in the uniqueness of ES cells: Oct4 and Nanog (Nichols *et al.* 1998; Chambers *et al.* 2003; Mitsui *et al.* 2003), and Stat3 and Sox2 (Matsuda *et al.* 1999; Masui *et al.* 2007). Recent studies have demonstrated that the forced coexpression of Oct3/4, Sox2, Klf4, and c-Myc induces reprogramming of mouse (Takahashi & Yamanaka 2006) and human somatic cells into pluripotent stem cells (iPS cells) (Takahashi *et al.* 2007).

Generally, the gene expression profile of a cell is considered to depend on its chromatin structure (Misteli 2001). The core unit of chromatin is the nucleosome, which is composed of a histone octamer

*Author to whom all correspondence should be addressed.
Email: katsutoshi.yoshizato@phoenixbio.co.jp
†Present address: Laboratory of Cell Engineering, Department of Molecular Biotechnology, Graduate School of Advanced Sciences of Matter, Hiroshima University, 1-3-1 Kagamiyama, Higashihiroshima, Hiroshima, 739-8526, Japan
‡Present address: Towa Environment Science Co., Ltd, ProPhoenix Division, 3-13-60, Kagamiyama, Higashihiroshima, Hiroshima 739-0046, Japan
§Present address: PhoenixBio Co., Ltd. 3-4-1, Kagamiyama, Higashihiroshima, 739-0046, Japan
Received 28 December 2007; revised 20 February 2008; accepted 27 February 2008.

consisting of two units each of four core histones, H2A, H2B, H3, and H4, and a 146-bp-long DNA sequence that wraps the histone octamer. Adjacent nucleosomes are connected together by linker DNA and histone H1. Recently, it has been reported that the major chromatin proteins such as core and linker histones, and heterochromatin protein 1 are uniquely associated in mouse ES cells, and that this is related to the highly plastic nature of their chromatin structures (Meshorer & Misteli 2006; Meshorer *et al.* 2006). Researchers have attempted to identify and characterize nuclear proteins specific to ES cells with large-scale proteomic analyses (Kurisaki *et al.* 2005; Nagano *et al.* 2005); however, the fine chromatin structures of ES cells remain largely unknown. The N-terminal tail domain of histone, also called the histone tail, protrudes from the surface of the nucleosome and is an important element in the functional state of chromatin. It is known that the histone tail interacts with the chromatin remodeling complex, which regulates transcriptional activity. Histone tails are biochemically modified through acetylation, methylation, phosphorylation, and ubiquitination which is essential for global transcriptional regulation (Turner 2002) and considered to be associated with epigenetic cell memory (Jenuwein & Allis 2001; Turner 2002).

In this study, we aimed to identify the nuclear proteins unique to ES cells. Nuclear proteins were prepared from mouse ES cells and subjected to affinity selection using histone tail peptides as baits. The tail peptide-associated proteins were identified and categorized into (I) chromatin remodeling proteins; (II) histone chaperones; (III) histone modification-related proteins; and (IV) others. Among them, we found that nucleoplasmin 3 (NPM3), a protein that belongs to the second category, is unique in that the protein was expressed at a higher level in undifferentiated ES cells compared with the ES cells that had been induced to differentiate toward neurons by retinoic acid (RA). NPM3 is a member of the nucleophosmin/nucleoplasmin (NPM) family (NPM1-3) that is ubiquitously present throughout the animal kingdom (Eirín-López *et al.* 2006; Frehlick *et al.* 2007). This family has important roles in cellular processes such as chromatin remodeling (Tamada *et al.* 2006), DNA duplication (Okuda 2002), and transcriptional regulation (Liu *et al.* 2007a). Importantly to our study, NPM 1 was reported to be involved in the proliferation of mouse ES cells and hematopoietic stem cells (Li *et al.* 2006; Wang *et al.* 2006). Thus, we characterized NPM3 further as to its role in the proliferation of ES cells. Our study indicates that NPM3 may play an important role in maintaining the unique chromatin structures of ES cells.

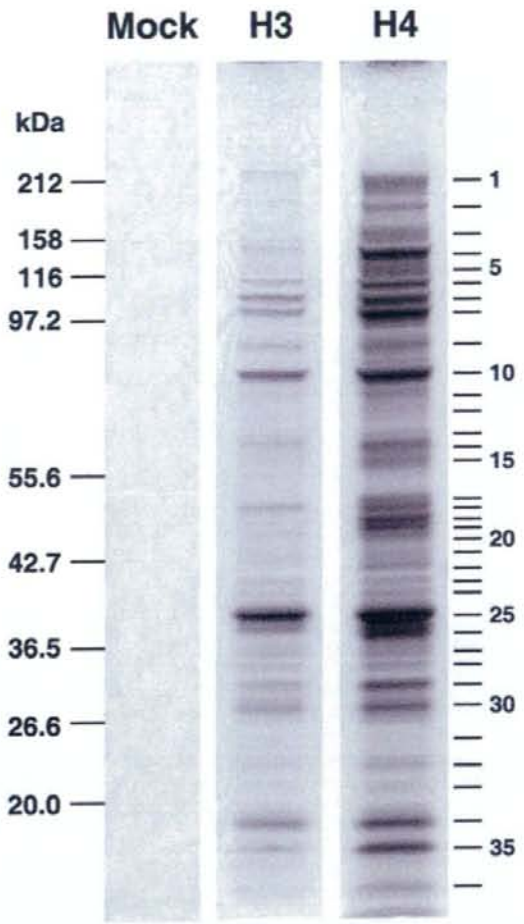

Fig. 1. Separation of histone tail-associated proteins by sodium dodecyl sulfate–polyacrylamide gel electrophoresis (SDS–PAGE). Nuclear extracts of CMT-1-ES cells were incubated with the beads bearing the H3 or H4 tail peptides. The binding experiments were carried out under the same conditions for both tail peptides. The bead-bound proteins were separated on 4–12% gradient SDS–PAGE and were stained with CBB R-250. The positions of molecular mass marker in kDa are indicated at the left side of the panel. The bands with Arabic numerals from 1 (top) to 36 (bottom) were cut off and subjected to protein identification by mass spectrometry. Identical banding patterns were observed in three independent analyses. 'Mock' represents a result using beads without histone tail peptides. There were no protein bands detected in the mock experiment, proving the specificity of protein binding to the beads.

Materials and methods

ES cell culture

Two types of mouse ES cell lines were used in this study: CMT-1-ES cells, which display a normal karyotype

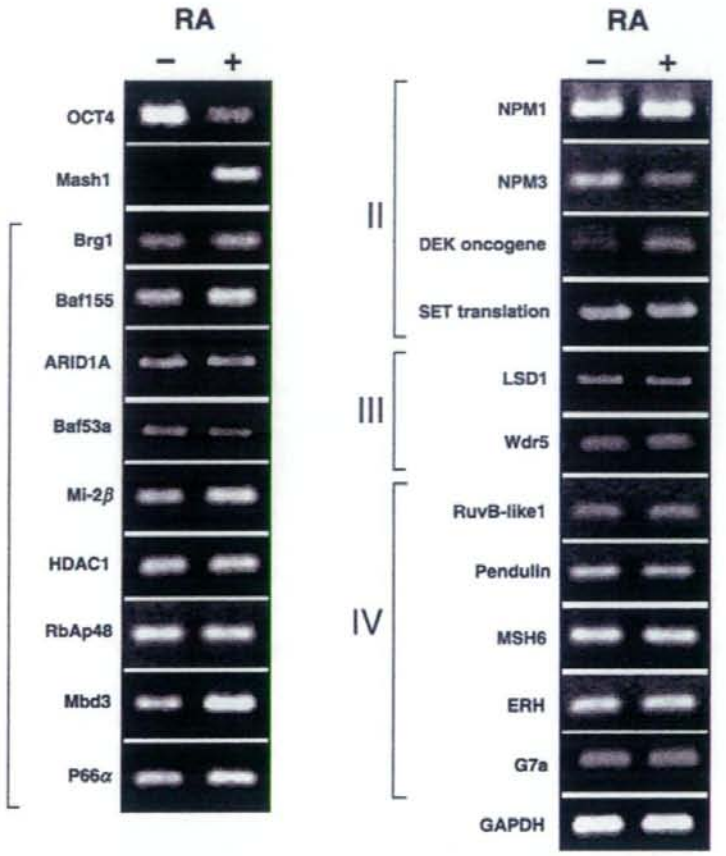

Fig. 2. Gene expression levels of histone tail-associated proteins in the undifferentiated and the differentiated embryonic stem (ES) cells. D3-ES cells were cultured for 120 h in the absence (−) and presence (+) of 0.5 μM retinoic acid (RA). RNA was extracted from both states of cells for semiquantitative reverse transcription–polymerase chain reaction (RT–PCR) to measure the expression levels of the indicated 20 genes. GAPDH (glyceraldehyde 3-phosphate dehydrogenase) gene was used as an internal control gene. The Roman numerals I to IV represent categories of nuclear proteins: I, chromatin remodeling proteins; II, histone chaperones; III, histone modification-related proteins; and IV, others. The experiments were independently carried out twice and similar results were obtained. A result of the two experiments is presented here. Similar results were also obtained from the experiment with CMT-1-ES cells.

and which preserve their original pluripotency in that they can be used for germ-line transmission when used according to the manufacturer's instructions (Cell & Molecular Technologies, New Jersey, NJ, USA), and D3-ES cells (ATCC, Manassas, VA, USA). These two types of ES cell are of the same origin (129/SV strain). We used CMT-1-ES cells for short-term culture experiments (up to 2 days; Figs 1 and 4A) in the presence of fetal bovine serum (FBS). D3-ES cells were used for long-term culture experiments (3–5 days, Figs 2 and 3), in which ES cells were characterized in terms of undifferentiated (RA-untreated) and differentiated (RA-treated) states. These cells were also used in experiments, in which the effect of NPM3 on the undifferentiated ES cells was examined in a long-term culture (3 days, Fig. 5). CMT-1-ES cells were cultured in high glucose Dulbecco's Modified Eagle Medium (DMEM) supplemented with 10% FBS and 1000 IU/mL LIF provided by Cell & Molecular Technologies on 0.1% gelatin-coated dishes. D3-ES cells were cultured on 0.1% gelatin-coated dishes in Glasgow's MEM (GMEM) supplemented with 10% KnockOut serum replacement (Invitrogen, Carlsbad, CA, USA), 1 × nonessential amino acids (Invitrogen), 1 mM sodium pyruvate, 0.1 mM β-mercaptoethanol (Sigma, St. Louis, MO, USA), 1000 IU/mL ESGRO (Invitrogen), and 1 μM ACTH (American Peptide Company, Sunnyvale, CA, USA; Ogawa *et al.* 2004). We confirmed that both types of ES cells showed similar characteristics in their expression profiles of mRNA and proteins, and the effects of RA on their expression (data not shown). Thus, ES cells are described simply as ES cells without referring to the original name of the cell lines (CMT-1 or D3) unless specified. Both types of ES cells were at 11 passages when purchased. ES cells were maintained without feeder cells and were used within four passage numbers. To obtain differentiated ES cells, D3-ES cells were cultured for up to 120 h in the presence of 0.5 μM RA (Sigma), under which ES cells are known to differentiate into neural

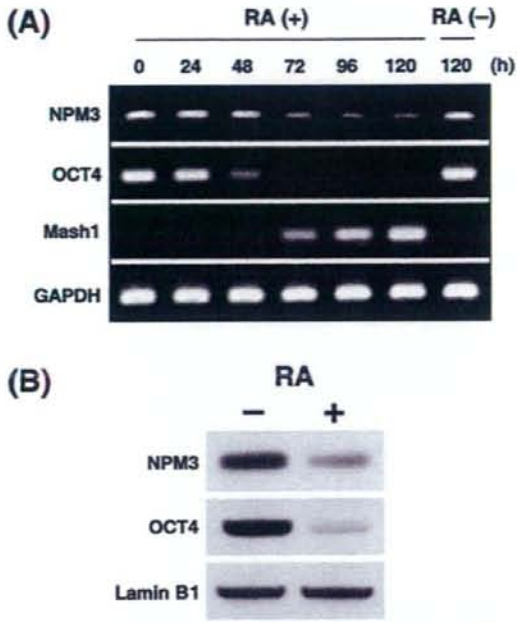

Fig. 3. Expression levels of nucleoplasmin 3 (NPM3) mRNA and protein during retinoic acid (RA)-induced differentiation. (A) mRNA expression. D3-ES cells were treated with 0.5 μM RA for up to 120 h and total RNA was isolated at the indicated time points for semiquantitative reverse transcription–polymerase chain reaction (RT–PCR) to estimate mRNA levels of NPM3, OCT4, and Mash1. GAPDH gene was used as an internal control gene. Similar results were also obtained from the experiment with CMT-1 cells. (B) Protein expression. D3-ES cells were cultured for 120 h in the absence (–) and presence (+) of 0.5 μM RA. Whole cell lysates were prepared for Western blotting of NPM3 and OCT4, and Lamin B1 as an internal control. Similar results were obtained from the experiment with CMT-1-ES cells.

precursor cells (Lee *et al.* 1994). LIF was removed from the culture media when cells were treated with RA.

Protein extraction and pull-down assay

Nuclear extracts of ES cells were obtained using a Nuclear Extraction Kit (Active Motif, Carlsbad CA, USA) according to the supplier's protocol. The 21-amino acid residue-long peptides (1–21 aa) starting from the N-terminus of the tail domain of histone H3 and H4 were purchased from Upstate (Charlottesville, MA, USA), which were biotinylated at the C-terminus. The peptides, 20 μg each, were incubated for 12 h at 4°C with 50 μL streptavidin-agarose beads included in a Pro-bound biotinylated pull-down kit (Pierce, Rockford, IL, USA). Nuclear extracts were dialyzed against phosphate-buffered saline (PBS) containing a complete ethylenediaminetetraacetic acid (EDTA)-free protease

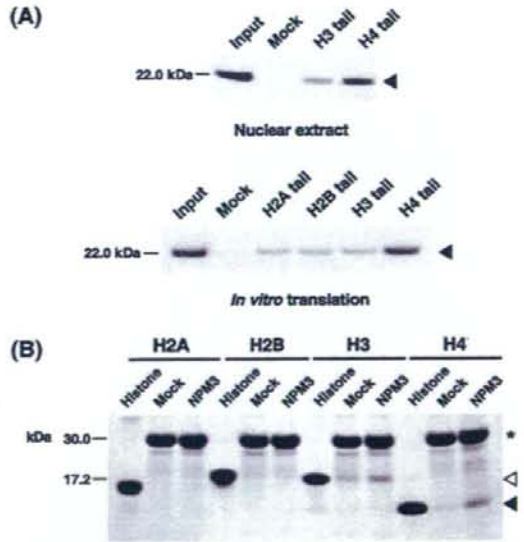

Fig. 4. Specificity of nucleoplasmin 3 (NPM3) binding to histone tails. (A) NPM3 binding to the tail domains of core histones. Upper panel. Nuclear extracts of CMT-1-ES cells were incubated with the beads bearing each of the tail peptides of histone H3 and H4. The proteins bound to the beads were subjected to Western blotting for NPM3. Lower panel. *In vitro* synthesized NPM3 was incubated with the beads bearing each of the tail peptides of H2A, H2B, H3, and H4. The proteins bound to the beads were processed as in the upper panel. 'Input' represents a Western blot of NPM3 in which the same amount of NPM3 as in the binding experiments was directly loaded on sodium dodecyl sulfate–polyacrylamide gel electrophoresis (SDS–PAGE) gels without incubation with beads. 'Mock' represents samples incubated with streptavidin-agarose beads that did not bind the tail peptides. The arrowhead at the right side of the gel points to NPM3 bands. The positions of the molecular mass (22.0 kDa) of NPM3 in kDa are indicated at the left side of the panel. (B) Binding of NPM3 with histone H2A, H2B, H3, and H4. Four types of histone each were incubated with anti-Flag M2 agarose beads on which *in vitro* synthesized Flag/NPM3 had been immobilized. The bound histones were separated by 4–12% gradient SDS–PAGE gels and visualized by CBB R-250. 'Mock' represents each histone incubated with anti-Flag M2 agarose beads that did not bind NPM3. 'Histone' indicates each calf thymus histone as loading markers. The asterisk at the right side of the gel points to immunoglobulin G (IgG) light chain bands that originated from anti-Flag IgG. The white and black arrowheads at the right side indicate the locations of histones H3 and H4, respectively. The positions of molecular mass markers in kDa are indicated at the left side of the panel. The graphs in A and B represent the results of one of the two independent experiments, which each showed similar results to the other.

inhibitor cocktail (Roche, Basel, Switzerland) for 12 h at 4°C and diluted with PBS to a final protein concentration of 1 mg/mL. The extracts, 500 μL each, were incubated with the peptide-linked streptavidin beads

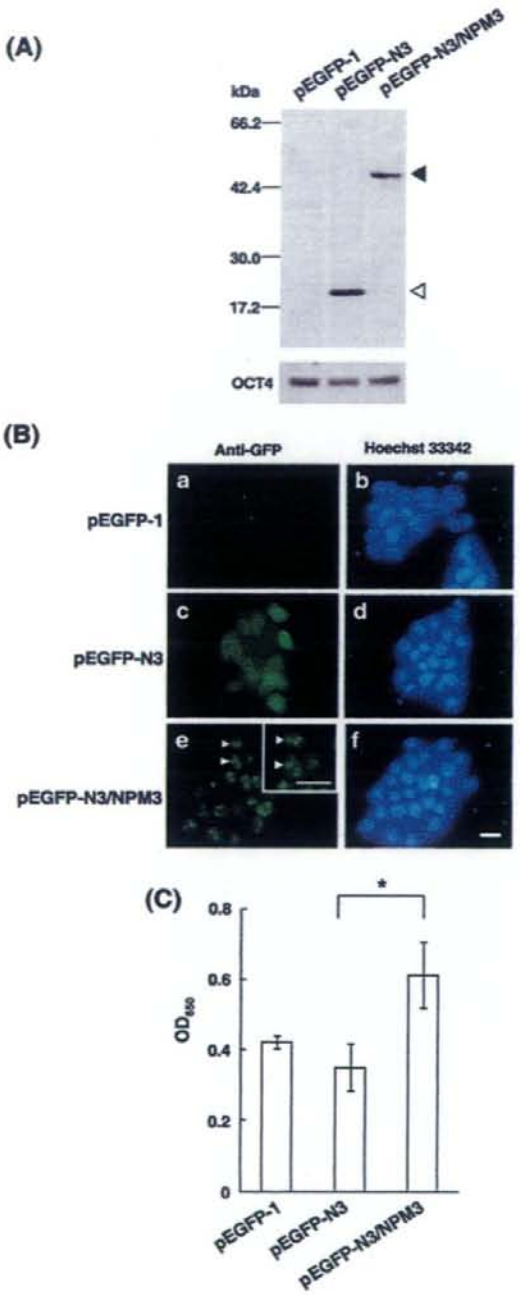

Fig. 5. Enhanced proliferation of nucleoplasmin 3 (NPM3)-overexpressing embryonic stem (ES) cells. D3-ES cells were transfected with each of pEGFP-1, pEGFP-N3, and pEGFP-N3/NPM3. (A) Western blot analysis of enhanced green fluorescent protein (EGFP)/NPM3 in transfected ES cells. Cell lysates were prepared from the transfected cells and subjected to Western blot analysis with anti-GFP antisera and with anti-OCT4 antibodies for checking the equal loading. The upper closed and lower open arrowhead at the right side point to the positions corresponding to the molecular masses of EGFP/NPM3 and EGFP proteins, respectively. The positions of molecular mass markers in kDa are indicated at the left side of the panel. (B) Localization of EGFP/NPM3 in ES cells. The transfected ES cells were subjected to immunocytochemistry using anti-GFP antibodies (a, c, e) and to Hoechst 33342 nuclear staining (b, d, f). EGFP/NPM3 proteins were localized in nucleoli (arrowheads in e), whereas EGFP protein was diffused in cytoplasm. The inset in e a magnified photo of a region including the cells indicated by arrowheads. Bar, 20 μm (C) Proliferation of the transfected cells. ES cells, 2×10^4 cells each, were placed in 96-well plates and transfected with pEGFP-1, pEGFP-N3, and pEGFP-N3/NPM3. The ES cells were allowed to proliferate for 3 days post-transfection and processed for 3-(4, 5-dimethylthiazolyl-2)-2, 5-diphenyltetrazolium bromide (MTT) assay. Student's *t*-test was used for statistical analysis for pEGFP-N3 vs. pEGFP-N3/NPM3. $^*P < 0.01$. The experiments of A through C were independently carried out three times, and each showed similar results to the others. The graphs in A and B represent the results of the three experiments.

for 12 h at 4°C. After washing with Tris-buffered saline (TBS), the beads were eluted by glycine-buffer (pH 3.0). The eluates were concentrated using a Biomax MW 5000 column (Millipore, Billerica, MA, USA), separated by 4–12% gradient NuPAGE (Invitrogen), and were visualized by Coomassie Brilliant Blue (CBB) R-250. CBB R-250 stained bands were cut off and trypsinized by in-gel digestion, and then the proteins were identified by mass spectrometry according to Yamagata *et al.* (2002).

RT–PCR analysis

Total RNA was extracted from ES cells by an RNeasy mini kit with DNase I-treatment (Qiagen, Valencia, CA, USA) and used to synthesize cDNAs using random hexamers using a Thermoscript kit (Invitrogen). The cDNAs were subjected to semiquantitative reverse transcription–polymerase chain reaction (RT–PCR) analysis using AmpliTaq Gold (Applied Biosystems, Foster City, CA, USA) with the gene-specific primers listed in Table 1. PCR products underwent electrophoresis on 1.5% agarose gels and were visualized by ethidium bromide. The band corresponding to the products of NPM3 gene was quantified using Image J (National Institutes of Health, Bethesda, MD, USA).

Construction of expression vectors and their transfection into ES cells

Fusion cDNA consisting of Flag-tag and the full-length of mouse NPM3 (Flag/NPM3) was amplified by PCR using KOD-Plus-Taq polymerase (TOYOBO, Osaka,

Table 1. List of primers used in reverse transcription–polymerase chain reaction

Gene	Primers	Expected product size (bp)
Mi2β	S: 5′-TGCTGCAACCACCCTTATCTC-3′ AS: 5′-AGTGGCCAGATTGATCCCAAG-3′	360
HDAC	S: 5′-GGCTGGCAAAGGCAAGTACTA-3′ AS: 5′-TTTCGTAAGTCCAGCAGCGAG-3′	302
RbAp48	S: 5′-AGGAGAAGTGAACAGGGCCC-3′ AS: 5′-AGACTCGTGGAGCAGATGCC-3′	352
Mbd3	S: 5′-GATGAATAAGAGTCGCCAGCG-3′ AS: 5′-AGGGTGCTGGTGTGTAGAGCA-3′	351
p66α	S: 5′-CACCCTTGAACCTGACCTAACG-3′ AS: 5′-GCTTTTCAAGAGCGCCTCAGT-3′	358
Brg1	S: 5′-CATCGCGCTCATCACATACCT-3′ AS: 5′-TCCGGTAGCTTGTTCTGCAG T-3′	393
Baf155	S: 5′-AAGGTGATCCAAGTCGCTCAG AS: 5′-ATTGCCATGGGTCGACTCTCT-3′	361
ARID1A	S: 5′-CAGATCAGAGGGCCAACCAT-3′ AS: 5′-CCGGACTTGAGGGACATCAT-3′	433
Baf53a	S: 5′-CAAGGCATTGTGAAATCCCC-3′ AS: 5′-CTTCAGGAATTTTCAGCCGC-3′	352
NPM1	S: 5′-TGGTCTTACGGTTGAAGTGTGG-3′ AS: 5′-CTCTTGACCCTTTGATCTCGGT-3′	380
DEK oncogene	S: 5′-CGTGAACAGCGAACTCGTGA-3′ AS: 5′-TCTTGGTGGTACTGCTGTCTGC-3′	368
SET translation	S: 5′-CATTCTGACGCAGGTGCTGAT-3′ AS: 5′-AGACCTCAAAACAGGGCGACT-3′	381
LSD1	S: 5′-GGTTCAGGTGTTTCTGGCTTG-3′ AS: 5′-GCAGCTGAATGACAACCTCCA-3′	403
Wdr5	S: 5′-CTGCCTG TAATAGTACCCAGCGT-3′ AS: 5′-GTTCTTCCTCTCCAACACTCAGC-3′	359
RuvB like 1	S: 5′-TGTGACCTTGCATGACCTGG-3′ AS: 5′-TGACACAGTTGCCTCGGTTG-3′	302
Pendulin	S: 5′-GCTCCAAGCTACTCAAGCTGCT-3′ AS: 5′-AACAGTGGGTCAATCGCACC-3′	351
MSH6	S: 5′-GGGCTAAGATGGAAGGTTACCC-3′ AS: 5′-AAGCCTCATGCACCTCTGTCTC-3′	351
ERH	S: 5′-GATGAATCCCAACAGCCCTTC-3′ AS: 5′-ACGGTGGCTTCAGAGTGACAA-3′	359
G7a	S: 5′-ACCTATGACCTCCCTACCCCA-3′ AS: 5′-TGGGTTCCATAGGGTGGTCTC-3′	303
NPM3	S: 5′-AACATGCTGTGCCTTACCGAG-3′ AS: 5′-GGAAGGATGCCACACAGCTTA-3′	302
OCT4	S: 5′-CTGAGGGCCAGGCAGGAGCACGAG-3′ AS: 5′-CTGTAGGGAGGGCTTCGGGCACTT-3′	485
Gapdh	S: 5′-GCACAGTCAAGGCCGAGAAT-3′ AS: 5′-GGTCATGAGCCCTTCCACAA-3′	355
Mash1	S: 5′-GGCTCAACTTCAGCGGCTTC-3′ AS: 5′-GTTGGTAAAGTCCAGCAGCTC-3′	350

Vector construction	
Primer	Sequence
NPM3-Flag-sense	5′-CGCGGATCCGCGCGGGGCGCTCACGGCCGT-3′
NPM3-Flag-antisense1	5′-GTCCTTGTAATCGCCGCCAGGCCTGCCCCTGTGCTT-3′
NPM3-Flag-antisense2	5′-CTAGTCTAGACTACTTGTCATCGTCGTCCTTGTAATCGCCGCC-3′
EGFP/NPM3-sense	5′-CGGAATTCCGGGGCGCTCACGGCCGTTTC-3′
EGFP/NPM3-antisense	5′-CGGGATCCAGGCCTGCCCCTGTGCTTCTT-3′

AS, antisense primers; S, sense primers.

Japan) and primer sets for Flag-tagged NPM3 (Flag/NPM3) described in Table 1. The PCR products were subcloned into the *Xba*I/BamH I sites in pDH105 vector (Hsu *et al.* 1998), which yielded pDH105-Flag/NPM3. Fusion cDNA consisting of enhanced green fluorescent protein (EGFP) and the full length of mouse NPM3 (EGFP/NPM3) was similarly amplified using EGFP/NPM3 primers described in Table 1. The products were subcloned into the EcoR I/BamH I sites in CMV (cytomegarovirus) minimum promoter-driven pEGFP-N3 vectors (Clontech, Palo Alto, CA, USA).

Embryonic stem cells (2×10^5 cells) in six-well plate were transfected for 24 h with promoter-less pEGFP-1 (Clontech), pEGFP-N3, or pEGFP-N3/NPM3 using Lipofectamine 2000 (Invitrogen). The ES cells were further cultured for 72 h and were harvested for analysis. Proliferation activity of the transfected cells was measured by 3-(4, 5-dimethylthiazolyl-2)-2, 5-diphenyltetrazolium bromide (MTT) assay using a Cell Counting Kit-8 (DOJINDO, Kumamoto, Japan) as changes of the optical density (OD) at the absorption wavelength of 450 nm against 650 nm.

Histone tail- and histone-binding assay for NPM3

The binding activity of NPM3 to histone tails was examined as follows. Mouse Flag/NPM3 was synthesized *in vitro* using a TNT SP6 Coupled Wheat Germ Extract System (Promega, Madison, WI, USA) and pDH105-Flag/NPM3. Biotinylated tail domain peptides of histone H2A (1–21 aa), H2B (1–22 aa), H3 (1–21 aa), and H4 (1–21 aa) were purchased from Upstate and 20 μg each were incubated with 50 μL streptavidin-agarose beads included in a Pro-bound biotinylated pull-down kit (Pierce) for 12 h at 4°C to obtain histone tail peptide-linked streptavidin beads. The streptavidin-agarose beads were incubated with biotin blocking buffer included in a Pierce's kit in control (mock control) experiments. Flag/NPM3 was diluted with TBS containing a complete EDTA-free protease inhibitor cocktail (Roche), 500 μL of which was incubated with the histone tail peptide-linked streptavidin beads for 12 h at 4°C. After being washed with TBS, the beads were treated with 2 × lithium dodecyl sulfate (LDS) sample buffer (Invitrogen) to elute the bound proteins. The eluates were subjected to Western blot analysis.

The binding activity of NPM3 to histones was examined as follows. Calf thymus histone H2A, H2B, H3, and H4 were purchased from Roche. Mouse Flag/NPM3 was diluted with TBS containing the Complete EDTA-free protease inhibitor cocktail (Roche), 500 μL of which was concurrently incubated with 10 μg of each of the histones and anti-Flag M2 agarose beads (Sigma) for 12 h at 4°C ('anti-Flag M2' represents the antibodies that generally recognize Flag-tag linked to proteins). The beads were washed with TBS three times and boiled with 50 μL 2 × LDS sample buffer (Invitrogen). The supernatants containing the bead-bound proteins were separated by 4–12% gradient NuPAGE (Invitrogen), and were stained with CBB R-250.

Western blot analysis for binding of NPM3 to histone tail, histone, and ES cell-lysate

Anti-mouse NPM3 rabbit antiserum was produced with synthetic C-terminal 12-amino acid residue-long peptides of NPM3. We verified the immuno-reactivity and immuno-specificity of the anti-NPM3 antiserum by Western blot analysis using *in vitro* synthesized NPM3 and other non-related proteins as antigens (data not shown). Western blot analysis for NPM3 binding was carried out using this antiserum on samples obtained from histone tail- and histone-binding experiments, and NPM3 gene-transfected ES cell lysates. Samples of the histone tail- and histone-binding experiments described above were separated by 4–12% gradient NuPAGE. NPM3 gene-transfected ES cells (2×10^5 cells) were directly lyzed in 1 × LDS sample buffer and were separated by 10% NuPAGE. These gels were transferred onto iBlot nitrocellulose membranes (Invitrogen). After blocking with 5% non-fat skim milk in TBS containing Tween 20 (TBST) for 1 h, the membranes were incubated with antirabbit NPM3 antiserum (1:1000 diluted), antirabbit GFP antisera (1:5000; Molecular Probes, Eugene, OR, USA), antirabbit OCT4 antibodies (1:1000; Santa Cruz Biotechnology, Santa Cruz, CA, USA) for 1 h at 37°C or overnight at 4°C. After being washed with TBST three times, the membranes were incubated with horseradish peroxidase-conjugated antirabbit IgG (1:1000; GE Healthcare, Buckinghamshire, UK) or horseradish peroxidase-conjugated antimouse IgG (1:1000; Vector Laboratory, Burlingame, CA, USA) for 1 h at 37°C. Signals were detected with ECL Western blotting detection reagents (GE Healthcare).

Immunocytochemistry

The transfected cells were fixed with 4% paraformaldehyde in PBS for 15 min at room temperature, and were permeabilized with 0.25% Triton X-100 in PBS for 10 min at room temperature. Plates were blocked in 5% BSA in PBS for 1 h at room temperature, and were then incubated with 1:750 diluted antimouse GFP antibodies (Chemicon, Temecula, CA, USA) overnight at 4°C. After being washed with PBST, the cells were incubated with 1:1000 diluted antimouse

IgG Alexa 488 (Molecular Probes) for 1 h at 37°C, washed with PBST, and were treated with Hoechest 33342 (Molecular Probes) for 10 min at room temperature for nuclear staining.

Results

Identification of histone tail-associated proteins

Nuclear extracts were prepared from ES cells and subjected to the pull-down assay using synthesized histone H3 and H4 tail peptides as baits. The proteins bound to baits were separated by sodium dodecyl sulfate–polyacrylamide gel electrophoresis (SDS–PAGE) (Fig. 1). Although the overall banding patterns were similar between the two baits, more proteins were bound to the H4 tail. Thus, in the following study, we focused on the H4 tail-associated proteins. Thirty-six bands were clearly discernible on the H4 tail gel and separable from each other, and were thus selected for identification by mass spectrometry. Five bands failed to produce meaningful mass spectra for sequencing. Altogether, we were able to identify 45 proteins from these bands. Twelve bands (numbers 3, 4, 7, 14, 15, 16, 19, 23, 25, 26, 28, and 31) comprised greater than two proteins (Table 2). These proteins were grouped into four categories, chromatin remodeling proteins, histone chaperones, histone modification-related proteins, and others (Table 2). Approximately a quarter of the proteins identified (10 proteins) were components of either of the two chromatin remodeling proteins, BAF (Brahma Associated Factor) complex (Wang *et al.* 1996a, b) that is known to act as a transcriptional activator (Carlson & Laurent 1994) or NuRD (nucleosomal remodeling and histone deacetylase) complex that acts as a transcriptional repressor (Zhang *et al.* 1999). There were five and two histone chaperones and histone modification-related proteins, respectively. The remaining 28 proteins were categorized as 'others'.

mRNA expressions of histone tail-associated proteins in undifferentiated and differentiated ES cells

In order to determine the biological significance of the histone tail-associated proteins, we compared mRNA expression levels of these proteins between undifferentiated (RA-untreated controls) and differentiated ES cells (RA-treated cells). For this purpose we selected 20 proteins from the above 45 proteins listed in Table 1: the nine chromatin remodeling proteins, the four histone chaperones, the two histone modification-related proteins, and the five from the other 28 proteins. 'Similar to BAF57' protein (number 16) in the chromatin remodeling proteins was not examined because of its uncertainty as a BAF member. Nucleolin (C23) (numbers 8–10) in the histone chaperones was omitted because of its ubiquitous expression in a variety of replicating cells (Tuteja & Tuteja 1998). The 24 proteins classified as 'others' were not examined because of their multifunctional or 'house-keeping' nature. The expression level of OCT4 and Mash1 were also determined as markers of undifferentiated and differentiated cells, respectively. Figure 2 shows mRNA expression levels of these 20 genes estimated by semiquantitative RT–PCR. The control ES cells expressed OCT4 at a higher level than the RA-treated cells as expected. The RA-treated ES cells, but not the untreated cells, expressed mRNA of Mash1, indicating that RA-treatment caused the cells to differentiate into neuronal progenitor cells as reported previously (Lee *et al.* 1994). Most of the genes were expressed at similar levels in both states of ES cells, or at higher levels in the RA-treated cells. However, NPM3 gene (protein 32 in Table 2) was exceptional: the expression level of the NPM3 gene was significantly (approximately 2.4-fold) higher in the undifferentiated ES cells than the differentiated cells relative to expression of a housekeeping gene (GAPDH) whose expression was similar in both control and RA-treated cells. The experiments to compare mRNA expression levels between the two types of ES cells were carried out twice and the same results were reproducibly obtained. Similar results were also obtained from the experiment with CMT-1-ES cells. Therefore, we concluded that NPM3 is a histone H4 tail-binding protein in ES cells and is associated with their undifferentiated state.

Expression of NPM3 mRNA and protein in ES cells during RA-induced differentiation

The above results (Fig. 2) suggested that expression of NPM3 is associated with the 'stemness' of ES cells and led us to further characterize the expression and biological role of this gene during RA-induced differentiation. ES cells were cultured for up to 120 h in the presence of 0.5 μM RA and the expression level of NPM3 was determined by semiquantitative RT–PCR together with the expression level of OCT4 and Mash1 gene as in Figure 2 (Fig. 3A). The expression profile of the NPM3 gene was similar to the OCT4 gene, which decreased during RA treatment, but different from that of the Mash1 gene, which was upregulated by RA at 72 h post-treatment, the expression level of which increased continuously thereafter. The NPM3 gene was expressed at a significant level up to 48 h post-treatment, started to decrease at 72 h,

ist of the identified histone-associated proteins

MW (kDa)	Protein	Accession	Category	Reference
219.0	Chromodomain helicase DNA binding protein 4 (Mi-2b)	gil39204553	Chromatin remodeling	–
181.9	Smarca4 protein (Brg1)	gil50927531	Chromatin remodeling	H4; Agalioti *et al.* 200
207.0	AT rich interactive domain 1A (ARID1A)	gil15808996	Chromatin remodeling	–
162.0	Cleavage and polyadenylation specific factor 1	gil16751835	Other	–
152.8	mutS homolog 6 (MSH6)	gil6754744	Other	–
123.8	Baf155	gil6678027	Chromatin remodeling	–
113.5	G7A	gil3986754	Other	–
192.0	Nucleoporin 133	gil20071177	Other	–
113.5	ADP-ribosyltransferase (NAD+, poly (ADP-ribose) polymerase) 1	gil20806109	Other	H3/H4; Pinnola *et al.* 2
88.2	Heterogenous nuclear ribonucleoprotein U	gil17390825	Other	–
95.9	LSD1	gil37360004	Histone modification	–
76.7	Nucleolin (C23)	gil128843	Histone chaperone	–
76.7	Nucleolin (C23)	gil128843	Histone chaperone	–
76.7	Nucleolin (C23)	gil128843	Histone chaperone	–
64.0	p66α (BC031407 protein)	gil23398610	Chromatin remodeling	H3/H4; Brackertz *et a*
–	NI	–	–	–
–	NI	–	–	–
55.0	Putative histone deacetylase1 (HDAC1)	gil2347180	Chromatin remodeling	–
29.2	U1 small nuclear ribonucleoprotein 70 kDa polypeptide A	gil26380180	Other	–
58.0	Pendulin (importinα1)	gil1363205	Other	–
50.9	Heterogenous nuclear ribonucleoprotein K	gil473912	Other	–
35.5	Similar to BAF57	gil51782778	Chromatin remodeling	–
43.4	DEK oncogene	gil29789160	Histone chaperone	–
50.5	RuvB-like protein 1 (Tip49a)	gil13435708	Other	–
42.6	β-tubulin	gil202229	Other	–
51.8	Chromatin assembly factor 1 subunit C (RbAp48)	gil2494893	Chromatin remodeling	H4; Verreault *et al.* 19
50.1	Elongation factor 1-γ	gil13626388	Other	–
50.2	Translation elongation factor eEF-1 α-chain-mouse	gil72870	Other	–
50.1	Elongation factor 1-γ	gil13626388	Other	–
47.4	BRG1/brm-associated factor 53A (Baf53a)	gil9789893	Chromatin remodeling	–
38.0	α-actin	gil49864	Other	–
41.0	γ-actin	gil809561	Other	–

ontinued

MW (kDa)	Protein	Accession	Category	Reference
22.5	Wdr5 protein	gil14250247	Histone modification	H3; Wysocka *et al.* 20
41.0	U5 snRNP-specific protein	gil21313414	Other	–
34.4	Heterogeneous nuclear ribonucleoprotein C	gil8393544	Other	–
30.9	Heterogeneous nuclear ribonucleoprotein A/B	gil6754222	Other	–
32.5	Nucleophosmin 1 (NPM1)	gil6679108	Histone chaperone	H3/H4; Okuwaki *et al.* Swaminathan *et al.* 2C
39.5	Similar to glyceraldehyde-3-phosphate dehydrogenase	gil28485300	Other	–
28.7	Eukaryotic translation elongation factor 1-δ	gil12963597	Other	–
31.8	Small nuclear ribonucleoprotein polypeptide A	gil13096860	Other	–
22.2	Histone 1, H1d	gil34328365	Other	–
28.3	Methyl-CpG binding domain protein 3 (MBD3)	gil23398550	Chromatin remodling	–
21.8	Histone 1, H1a	gil21426823	Other	–
24.7	Elongation factor 1-β homolog	gil5902663	Other	–
–	NI	–	–	–
33.4	SET translocation	gil13591862	Histone chaperone	H3/H4; Kawase *et al.* Muto *et al.* 2007
23.9	Small nuclear ribonucleoprotein B	gil6678053	Other	–
19.4	Nucleoplasmin 3 (NPM3)	gil6679110	Histone chaperone	–
–	NI	–	–	–
15.1	Histone H2B	gil280961	Other	H3/H4; Ilyin & Bayev
14.0	Small nuclear ribonucleoprotein D3	gil13385598	Other	
12.4	Enhancer of rudimentary homolog (ERH)	gil6679685	Other	

ified proteins are categorized into chromatin remodeling proteins, histone modification related-proteins, histone chaperones, and others. 'NI' represents the t were not identifiable. The numbers in the third right column (Accession) indicate protein database accession numbers. Literatures are cited in 'Reference' that ed to directly bind to histone H3 and/or H4.

and continued to decrease thereafter. The expression level of NPM3 protein together with that of OCT4 protein in both control and RA-treated cells was estimated by Western blotting on whole cell lysates (Fig. 3B). As expected, ES cells in the undifferentiated state, but not in the differentiated state, showed robust expression of NPM3 and OCT4 protein.

Histone binding activity of NPM3

To characterize binding specificity of NPM3 protein toward the tail domain of core histones, we carried out two types of *in vitro* binding experiments using nuclear extracts of ES cells as a source of the native NPM3 (Fig. 4A, upper panel) and *in vitro* synthesized Flag/NPM3 (Fig. 4A, lower panel). The baits were the tail peptides of histone H3 and H4, and those of histone H2A, H2B, H3, and H4 in the former and the latter binding experiments, respectively. Native NPM3 in the nuclear extracts showed a much higher affinity to the H4 tail peptide than the H3 tail peptide, which supported the previous result (Fig. 1). The *in vitro* synthesized NPM3 also had a high affinity to the H4 tail.

To examine the influence of other domains of histone molecules on the binding of NPM3 to the tail domain, we estimated its binding to whole histone molecules. The histone molecules tested for binding were H2A, H2B, H3, and H4. Flag/NPM3 was incubated with anti-Flag M2 agarose beads and each of the histones. The bead-bound histones were separated by SDS–PAGE (Fig. 4B). No signals of bound histone were observed for histone H2A or H2B. Interestingly, not only histone H4, but also H3 bound to the immobilized NPM3, although the tail domain of H3 alone did not show or showed very little binding activity for the protein (Fig. 4A).

Overexpression of NPM3 gene in ES cells

In order to discover the biological significance of the binding of NPM3 to histone H4 and likely to H3, we investigated the effect of NPM3 overexpression on ES cells. ES cells were transfected with pEGFP-N3/NPM3, together with pEGFP-1 and pEGFP-N3, both as control genes, and were allowed to proliferate for 3 days. Observation via a fluorescence microscopy indicated that the transfection efficiency was about 70%. The expression of the fusion protein, EGFP/NPM3, was verified by Western blot analysis with anti-GFP antisera (Fig. 5A). Overexpression seemed not to affect the pluripotent nature of ES cells, because NPM3-overexpressing ES cells expressed OCT4 (Fig. 5A) and Nanog (data not shown), both pluripotent marker proteins, at levels similar to those observed in control cells. Immunocytochemistry for EGFP/NPM3 showed that NPM3 was distributed in both nucleoli and nuclei (Figs 5B.e and its inset) as reported previously (Huang *et al.* 2005). NPM3 was more concentrated in nucleoli than in nuclei.

NPM1 belongs to the same family as NPM3 and is involved in the regulation of proliferation of mouse ES cells and hematopoietic stem cells (Li *et al.* 2006; Wang *et al.* 2006). Therefore, we compared the proliferation rate among the three types of transfected cells by MTT assay (Fig. 5C). The rate of proliferation of NPM3-overexpressing ES cells was significantly increased by about 1.5-fold over both of the control transfectants ($P < 0.01$). This increase was confirmed by direct cell counting at a level of $P < 0.05$ (data not shown).

Discussion

Nuclear properties and chromatin structures of ES cells have received intensive scrutiny (Meshorer & Misteli 2006; Meshorer *et al.* 2006). Microarray (Kelly & Rizzino 2000; Ramalho-Santos *et al.* 2002) and proteomic analyses are comprehensive and powerful approaches to characterize and further understand self-renewal and pluripotency of ES cells at the gene and protein levels (Guo *et al.* 2001; Kurisaki *et al.* 2005; Nagano *et al.* 2005; Wang & Gao 2005; Baharvand *et al.* 2006; Stanton & Bakre 2007). Our pull-down assay was made on the nuclear proteins of ES cells using synthetic peptides of histone tail domain as baits, because the histone tail domain is considered to play critical roles in the biological functions of histones, not least because histones incorporate target sites for active biochemical modifications that profoundly affect their function. It should be noted that the used baits were synthetic unmodified ('bare') histone tail peptides. The synthetic tails are likely not to receive such modifications, because cofactors necessary for enzymatic modifications of histone such as acetyl-CoA might be lost during preparation. Despite this limitation, we were able to isolate the histone binding proteins that included more than 10 previously reported proteins as histone binding proteins.

Histone H3 and H4 tail peptides showed similar binding profiles toward nuclear proteins. However, the histone H3 tail bait demonstrated a lower binding affinity to most of the proteins relative to the histone H4 tail bait, although the reason for this difference was not elucidated and will require further study. Forty-five proteins were identified as candidates that associate with the histone H4 tail and these were grouped into four broad categories: chromatin

remodeling proteins, histone chaperones, histone modification-related proteins, and others. It is noteworthy that members of the two chromatin remodeling complexes, BAF (Wang *et al.* 1996a, b) and NuRD complex (Zhang *et al.* 1999) were among the most abundant proteins identified. RbAp48 and p66α of them were reported to directly associate with histone H4 (Verreault *et al.* 1998; Brackertz *et al.* 2006). The present study suggests that these chromatin remodeling proteins are significant for differentiation rather than maintenance of pluripotency of ES cells because they were upregulated in the RA-treated ES cells. Five proteins were identified as histone chaperones including NPM3, which is a member of the NPM family (Macarthur & Shackleford 1997; Shackleford *et al.* 2001; Frehlick *et al.* 2007). Histone chaperone directly regulates the chromatin structures (Adkins & Tyler 2004; Tamada *et al.* 2006; Frehlick *et al.* 2007). For example, HIRA, a chaperone of histone H3.3, regulates the binding of histone H3.3 with chromatin in mouse ES cells (Meshorer *et al.* 2006). Histone H3 and H3.3 are thought to be in a dynamic state as to the binding to chromatin in HIRA-knockout ES cells: they are in either an unbound or a more loosely bound state compared with the wild-type cells. This dynamic state of the chromatin structure might be responsible for the observed accelerated differentiation to neurons of the knockout cells. The histone chaperones identified in the present study might be responsible for maintaining the chromatin structures unique to ES cells. It should be noted that NPM3 has not been characterized as a histone H4 tail-binding protein and only this protein was highly expressed in undifferentiated ES cells among the identified proteins in the present study.

Together with NPM1 and NPM2, NPM3 belongs to the NPM family that has important roles in cellular processes such as chromatin remodeling, genome stability, ribosome biogenesis, DNA duplication and transcriptional regulation (Philpott *et al.* 1991; Savkur & Olson 1998; Okuda 2002; Grisendi *et al.* 2005; Huang *et al.* 2005; Tamada *et al.* 2006; Liu *et al.* 2007a, b). NPM1 rapidly increases its expression in response to mitogenic stimuli and is highly expressed in tumor and growing cells (Chan *et al.* 1989; Nozawa *et al.* 1996; Grisendi *et al.* 2006). NPM1 preferentially binds to histone H3 and mediates the nucleosome assembly (Okuwaki *et al.* 2001; Swaminathan *et al.* 2005). NPM2 also binds to histone H2A and H2B, and mediates chromatin assembly of sperms (Dilworth *et al.* 1987; Philpott *et al.* 1991; Tamada *et al.* 2006). The least amount of data are available for NPM3, which is the most recently identified as a NPM3 family member.

Nucleoplasmin 3 was originally identified among the genes activated by mouse tumor virus proviral insertions (Kuriki *et al.* 2000). In human tissues, NPM3 was ubiquitously expressed, preferentially in the pancreas and the testis (Shackleford & Macarthur 2001). It was reported that an antisense oligonucleotide of NPM3 blocks the decondensation of sperm chromatin in fertilized mouse eggs (Mclay & Clarke 2003). Our results demonstrate that NPM3 is capable of binding to the histone H4 tail domain. mRNA and proteins of NPM3 were expressed in the undifferentiated ES cells at higher levels than in the differentiated ES cells. We consider that NPM3 may be a key molecule responsible for maintaining chromatin structures unique to ES cells. NPM3 showed a lower affinity to the H3 tail domain compared with the H4 tail domain under the conditions used in our binding experiments. However, there was no such significant difference in the affinity to NPM3 when tested using the whole histone H3 and H4 molecules. Therefore, it is likely that NPM3 binds to domains of histone H3 other than the tail, or other domains are required for the NPM3 binding to the tail domain.

Nucleoplasmin 3 has been implicated in ribosome biogenesis, which is involved in cell proliferation (Huang *et al.* 2005). Thus, it is plausible that NPM3 stimulates proliferation of ES cells through regulating chromatin structure of the rRNA gene. This possibility appears to be consistent with the nucleolar distribution of NPM3 as suggested by Huang *et al.* (2005). There is still another possibility about the mechanism of stimulation of ES cells by NPM3. NPM1 stimulates the proliferation of mouse ES cells (Wang *et al.* 2006). In addition, it has been reported that NPM3 directly interacts with NPM1 (Huang *et al.* 2005). Our preliminary experiments also showed that NPM3 forms a complex with NPM1 in mouse ES cell lysates (data not shown). Therefore, it is most likely that NPM3 regulates the ES cell proliferation through interaction with NPM1 and possibly with other cell cycle regulators.

As a preliminary study, we made NPM3 gene knock-down experiments with mouse ES cells under conditions that had been commonly used in the gene knock-down study with ES cells. However, these trials were unsuccessful. Instead, we successfully knocked-down NPM3 genes in P19 cells, a mouse embryonal carcinoma cell line. These downregulated cells showed no alterations of phenotypes as to proliferation and expressions of Nanog and OCT4 genes. Thus, it is strongly suggested that other protein(s) will compensate NPM3 as its role in proliferation of ES cells if NPM3 gene knock-down ES cells would be successfully generated.